Single Trial Recognition of Anticipatory Slow Cortical Potentials: The Role of Spatio-Spectral Filtering

Gangadhar Garipelli, Ricardo Chavarriaga, José del R. Millán

***Abstract*— Single trial recognition of slow cortical potentials (SCPs) from full-band EEG (FbEEG) faces different challenges to classical EEG such as noisy, high magnitude ($\sim \pm 100\,\mu V$) infra slow oscillations (ISO) with f $\leq$ 0.1 Hz and high frequency spatial noise from a variety of artifacts. We analyze offline the anticipation related SCPs recorded from 11 subjects over two days in a variation of the Contingent Negative Variation (CNV) paradigm with *Go* and *No-go* conditions in an assistive technology framework. The results suggest that widely used spatial filters such as Common Average Referencing (CAR) and Laplacian are sub-optimal for the single trial analysis of SCPs. We show that a spatial smoothing filter (SSF), which in combination with CAR enhances the spatially distributed SCP while attenuating high frequency spatial noise. We report, first, that a narrow band filter in the range $[0.1\ 1]$ Hz captures anticipation related SCP better and effectively reduces ISOs. Second, the SSF in combination with CAR outperforms CAR-alone and Laplacian spatial filters. Third, we compare linear and quadratic classifiers calculated using optimally filtered Cz electrode potentials and report that the best methods resulted in single trial classification accuracies of $83 \pm 4\%$, where classifiers were trained on day 1 and tested using data from day 2, to ensure generalization capabilities across days (1-7 days).**

I. INTRODUCTION

Slow cortical potentials (SCPs) are positive or negative deflections observed in electroenchephalogram (EEG) and magnetoencephalogram (MEG) lasting from about a third of a second to several seconds with magnitudes up to $50\,\mu V$ [1]. Self-regulation of SCPs has been suggested to be useful not only for brain-computer interaction (BCI) for severely paralyzed patients [1], but also for treating attention deficit hyperactivity disorder and monitoring various psychiatric conditions such as schizophrenia and depression [2]. However, since the demonstration of SCP as a control signal for BCI devices [1], there have not been numerous replications compared to other control signals such as sensory-motor rhythms (SMR), P300 potentials and steady-state visual evoked potentials (SSVEP) [3]. This is probably due to the fact that the use of SCP-based BCI faces different challenges compared to classical BCIs, such as: 1) the requirement of a reliable full-band EEG (FbEEG) hardware (direct current coupled) [4], 2) tedious training sessions ranging from several months to a few years [1], 3) the elusive nature of cognitive phenomena underlying the SCPs and 4) the fact that SCPs are spatially distributed oscillations covering large scalp areas and are vulnerable to a variety of artifacts (e.g, Infra Slow Oscillations (ISOs), changes of skin-conductance, Electrooculogram, tongue/head/facial muscle movement, etc. [4]). It is necessary to overcome all these challenges to build a reliable SCP based BCI.

In previous work, we presented fast and reliable techniques for offline single trial classification [5] and reported the possibility of recognizing anticipation related SCP in an online experimental set-up [6]. Those studies were based on a small pool of subjects trained and tested using the recordings on the same day. Also, the protocols were designed using flashes similar to the standard the contingent negative variation (CNV) protocol and were less application oriented.

In this paper we present our latest attempts to address the above challenges and report offline results on single trial recognition of anticipation related SCPs recorded from 11 healthy subjects on two different days. We recorded the FbEEG using a variation of CNV *Go* and *No-go* paradigm in a realistic assistive technology based framework for a web-browsing application [5], [7], [8]. More specifically, we first *spectrally localize* the anticipation related potentials and then, compare state-of-the art techniques for *spatial filtering* (e.g. Laplacian and common average reference, CAR) with a spatial smoothing filter (SSF) by comparing separability of feature distributions. Finally, for the best spatial and spectral filter combination, we report a comparison of the classification performances of linear and quadratic classifiers calculated using Cz electrode potentials, where the anticipation related SCP is more prominent. To ensure generalization capabilities over days, the classifiers were trained using recordings of day 1 and tested on recordings of day 2.

In the following Sec. II, we present the experimental set-up and FbEEG acquisition, spatio-spectral filtering techniques and classification methods. In Sec. III, we present the results of spectral localization, followed by comparison of spatial filters using a separability index and single trial classification results obtained using linear and quadratic classifiers. Finally, in Sec. IV, we discuss the current results and suggest some future directions.

II. METHODS

A. Experimental set-up

The protocol for recording anticipation related SCP was designed in the framework of an assistive software for web browsing by icon selection with an auto-scanning mode as shown in Fig. 1 (the scanning of icons is similar to that of [8]). The protocol is a variant of the CNV paradigm with Go and No-go conditions [5], [7], in which one or more contingent warning stimuli predicts an imperative stimuli.

Authors are affiliated to Defitech Chair in Non-Invasive Brain-Machine Interface, Center for Neuroprosthetics, School of Engineering, École Polytechnique Fédérale de Lausanne (EPFL), Switzerland, CH-1015. e-mail: gangadhar.garipelli@epfl.ch

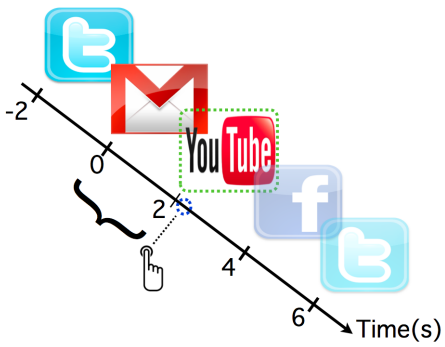

Fig. 1. Timeline of events in the anticipation based web-browsing protocol. A cue presented 2 s prior to the beginning of each scan predicted the target icon. In each scan, the icons were highlighted with 2s interval sequentially resulting in a trial. In this figure, the *YouTube* icon is the target icon. The *Go* trial corresponded to the time window from the highlight of the *Gmail* icon at 0 s until highlight of the *YouTube* at 2 s. All icons were visible throughout the experiment.

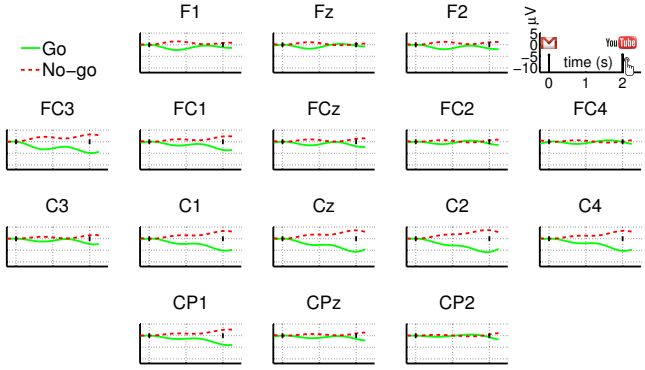

Fig. 2. Grand average of potentials computed at different electrode sites for *Go* and *No-go* trials using the recordings of subject 3 (with spectral filtering of $[0.1\ 1]\,Hz$ and referenced to CAR). Similar plots were found for the remaining subjects.

Firstly, a cue presented 2s prior to the beginning of each scan revealed the target icon. In each scan, the icons were highlighted sequentially every 2s. Each window of highlight corresponds to a trial. Each scan contained one *Go* trial and up to 3 *No-go* trials. The subjects were informed to press a button quickly on the highlight of target icon by anticipating from the moment of the highlight of the pre-target icon with their preferred hand. The time window from the pre-target icon highlight to the target icon highlight resulted in a *Go* trial. If the succeeding icon was not a target icon, the subjects were instructed to do nothing (*No-go* trial). The feedback of reaction time (RT) and a corresponding web-page of the target icon were presented to the subjects if the RT met a criteria $RT \leq \pm 100$ ms after a target icon highlighted. If the criteria was not met, the scan finished approximately 1 s after the feedback of RT only. To minimize artifacts, the subjects were instructed to fixate their eyes on a cross presented in the center of the computer screen and to avoid any other movements such as facial muscle, tongue and head.

B. EEG acquisition and ERP analysis

We recorded FbEEG of 11 healthy human subjects (aged 26.4 ± 2.4 years, 1 female, all right handed) with an average of 123 ± 28 *Go* trials and 264 ± 68 *No-go* trials per subject per day over two different days (with a gap of 1-7 days). FbEEG was acquired with 64 electrodes according to the international 10-20 standard at 2 KHz sampling rate, using the Biosemi EEG hardware (with full-DC and 400 Hz lowpass cut-off). The data was decimated to 64Hz for the offline analysis.

We extracted trials with $[0\ 2.5]$ s windows synchronized to the highlighting of icons and labeled accordingly (c.f. Fig. 1). For further analysis, we discarded all the trials that had the magnitude of any electrode above $100\,\mu$V that were suspected to be artifacts. The data was baseline corrected using the sample at 0 s. Using grand averages, we report the presence of the well known CNV potential: an increasing negativity at central electrodes (mainly Cz) for the *Go* condition [5], [6], [7] and an almost flat or slightly positive response for the *No-go* condition (c.f. Fig. 2).

C. Spectral and spatial filtering

The *Go* and *No-go* grand-averages are clearly separated but the single trials suffer very high variability due to noisy high amplitude ISOs and high-frequency spatial noise (i.e. adjacent electrodes contain a very different SCP trends). To address this variability we study both spectral and spatial filtering using the discriminability of *Go* and *No-go* trials. To achieve a better SNR we explore various narrow band filters (using zero phase FIR filters with order N=10 x sampling frequency for ensuring sharp transition; designed using `fir1`, applied using `filtfilt` routines of Matlab, *Mathworks Inc. USA.*) with passband of $[0\ 5]$ Hz, $[0.01\ 5]$ Hz, $[0.01\ 1]$, $[0.05\ 1]$ Hz, $[0.1\ 1]$ Hz, $[0.5\ 1]$ Hz, $[0.5\ 2]$ Hz, $[0.5\ 2]$ Hz and $[0.5\ 3]$ Hz.

We compare spatial filters such as CAR, Laplacian filter and spatial smoothing filter as well as no spatial filtering for each spectral band (c.f. Sec. III). Given a recording at the i^{th} electrode, $e_i(t)$, the Laplacian filtered data was computed as $e^{Laplace}(t) = e_i(t) - \sum_j^K \frac{1}{K} e_j(t)$. Where K is the number of neighboring electrodes (=4) electrodes chosen in 'plus (+)' configuration as described in [9]. We test a spatial filter called Spatial Smoothing Filter (SSF), which corresponds to the spatial convolution of EEG data with a Gaussian kernel. The $e_i^{SSF}(t) = \sum_j^K w_{ij} e_j(t)$, where $w_{ij} = exp(-\frac{d_{ij}^2}{2\sigma^2})$ and d_{ij} is the Euclidean distance between electrodes i and j in 3D coordinate system. The key difference from the Laplacian filter is that, the Laplacian filter removes a fraction of activity of adjacent electrodes whereas the SSF enhances the shared activity. In the current paper, for the analysis of SSF we chose electrodes in the same configuration as the Laplacian filter to allow a fair comparison (we set $\sigma = 0.15$ resulting in same magnitude of weights than Laplacian for the first neighbors, but with opposite sign). Such Gaussian kernel based smoothing filters are widely used in the analysis of functional magnetic resonance imaging (fMRI) data [10]. But to the best of our knowledge, these filters were not explored in the analysis of SCP in FbEEG.

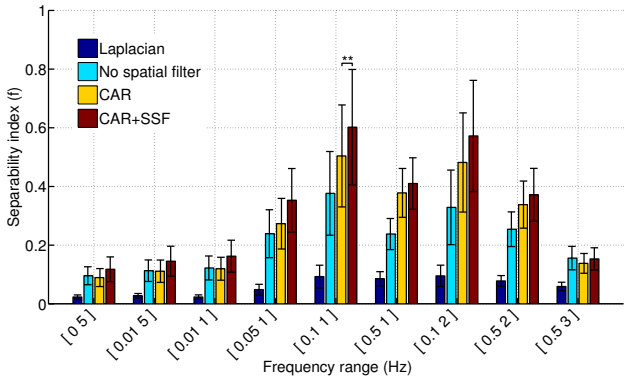

Fig. 3. The separability index f compared for various spatial and spectral filters for all subjects. For the best spectral filter $[0.1\ \ 1]Hz$, the CAR+SSF outperfrom CAR alone (Wilcoxon, p=0.01).

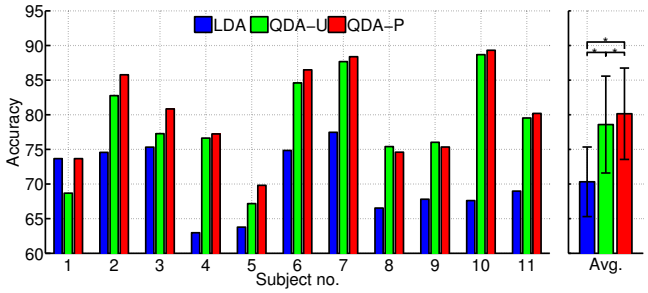

Fig. 4. Single trial classification accuracies for LDA and QDA classifiers for 11 subjects. Blue bars represent LDA classifiers, green bar refers to QDA classifiers with uniform prior (QDA-U) and red bars with prior proportional to the number of samples per class (QDA-P). The performances of LDA, QDA-U and QDA-P are significantly different (Wilcoxon, $p = 0.05$).

D. Feature selection and classification

In the current report, we restrict our studies to features computed from Cz electrode, under which the anticipation related SCPs are more prominent [5], [6], [7].

For each trial, the Cz potentials at 8 equally spaced time points (i.e, at 0.25s, 0.5s, ... 2.0 s) are chosen as a feature vector, $x = [e_{Cz}(T_1)\, e_{Cz}(T_2)\, \ldots\, e_{Cz}(T_8)] \in R^8$ where, T_k represents the k^{th} time point. We assume that these features for each class follow unimodal Gaussian distributions. These feature vectors are used to compute a separability index as well to train and to test the Linear Discriminant Analysis (LDA) classifiers and Quadratic Discriminant Classifiers (QDA). To compute the separability index, the feature vectors are first projected into a canonical space $y \in R$ by using $y = \mathbf{W}^T x$ for better separation (the projection matrix $\mathbf{W}$, maximizes the between-class variance whilst simultaneously minimizing the within-class variance [11]). Using the projected data, the separability index is defined as $f = \frac{(\mu^{Go} - \mu^{Nogo})^2}{(\sigma^{Go})^2 + (\sigma^{Nogo})^2}$, where μ and σ are mean and standard deviation computed from the canonical space for both *Go* and *No-go* trials. The LDA classifier is calculated by computing a threshold in the canonical space (described above) based on sample balance to separate the classes ($\theta = \mu^{Go}\eta^{Nogo} + \mu^{Nogo}\eta^{Go}$, where μ are means in canonical space an η are the proportion of Go and No-go trials). The projection matrix and threshold are calculated using data from day 1.

For a QDA classifier, the feature vector x, the posterior probabilities $p(\mathcal{C}_{Go}|x)$ and $p(\mathcal{C}_{Nogo}|x)$, are computed using Bayes' formula. As opposed to LDA, QDA does not assume a pooled covariance matrix and hence forms a quadratic decision boundary [11]. For obtaining the likelihood for x, the mean vectors and covariance matrices for each class are computed from the training data. The prior probabilities are set either to be uniform or to the proportion o *Go* and *No-go* samples of training data.

III. RESULTS

Firstly, we compare various spectral and spatial filters as described in Sec. II-C using the separability index (c.f. Sec. II-D) computed using recordings of day 1. From Fig. 3, it can be seen that the *Go* and *No-go* conditions are maximally discriminant in the frequency range $[0.1\ 1]$ Hz for most of the spatial filter types. No statistical differences observed for the filters with passband $[0.1\ 1]$ Hz and $[0.1\ 2]$ Hz. However, further spectral deviation results in a decreasing trend in the separability index. Meaning, the inclusion of wider spectral range is likely to result in increased noise and therefore not favorable for robust classification. The requirement of a high pass at 0.1 Hz is likely due to the ISOs which lie below that frequency contribute more to the noise than the task specific features in the current experiment. Furthermore, in the current experiment the anticipation related potentials are observed as an increasing negativity within the window of 2 s with an approximate linear trend. The spectral content of such a feature is likely to be less than 1 Hz.

Secondly, we compare various spatial filters (CAR, Laplacian, CAR+SSF and no spatial filtering) for the best spectral filter, $[0.1\ 1]$ Hz, that provided best feature separation (c.f. Fig. 3). From the figure it can be inferred that referencing to CAR enhances the SNR as compared to no spatial filter, which is likely because CAR removes global activity (external sources such as EOG, EMG, etc.). Interestingly, the Laplacian filter underperforms in comparison to no spatial filter. This is likely due to the fact that SCPs are spatially broadly distributed activities and shared among several neighboring electrodes, and Laplacian by design reduces it. On the contrary, in combination with CAR the SSF takes advantage of this fact and results in the best scores. In other words, since the SSF is a weighted summation of neighboring activity, enhances the common component (signal) and attenuates local variability (noise; assumed zero mean).

Third, we compare single trial classification accuracies using LDA and QDA classifiers for the best spatial and spectral filter combination, i.e. for $[0.1\ 1]$ Hz spectral filter and in combination with CAR and SSF (c.f. Fig. 4). In the case of QDA classifiers, we compare accuracies for two prior probability settings: uniform (QDA-U) and the proportion of number of training samples per class (QDA-P). The classifiers were trained using data recorded on day 1

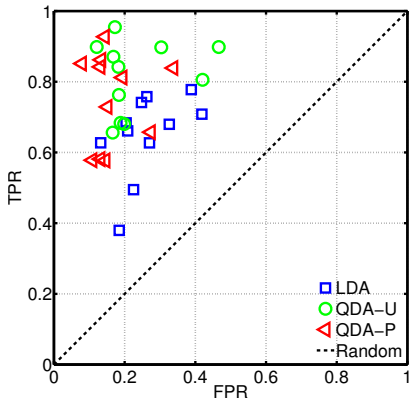

Fig. 5. The accuracy in the ROC space for LDA (in blue squares) and QDA classifiers. Each symbol represents one subject. The green circles refer to QDA classifiers with uniform prior (QDA-U) whereas the red triangles refer to QDA with prior proportional to number of samples (QDA-P).

and tested using day 2. As seen in Fig. 4 the mean accuracy for LDA classifiers across 11 subjects is 73±4% with a minimum of 64% (subject 5) and a maximum of 77% (subject 7). The QDA-U results in an average accuracy of 80±5% with an improvement of 7% over LDA (Wilcoxon, $p = 0.05$), a minimum classification of 67% (subject 5) and a maximum of 88% (subject 10). A further improvement of 3% in classification accuracy (83±4%) is obtained by more accurate priors of QDA-P (Wilcoxon, $p = 0.05$). The QDA-P performed with minimum accuracy of 69.5% (subject 5) and maximum accuracy of 89% (subject 10). Overall, this improvement is achieved by reducing the false positive rate (FPR) which is favorable for the current application (c.f. Fig. 5).

IV. CONCLUSIONS AND FUTURE WORKS

We presented a BCI framework based on single trial recognition of SCPs related to anticipatory behavior. We recorded FbEEG of 11 subjects in two different days using an assistive technology framework for web-browsing. From the offline analysis we found that a narrow band spectral filter with a passband of $[0.1\ 1]$ Hz in combination with CAR and SSF results in the best feature separability. For this combination, we compared classification accuracies of LDA and QDA classifiers calculated using features computed from Cz electrode potentials at 8 different time points within a 2s window. To ensure generalization capability across days, the classifiers were trained using day 1 and tested using day 2 (with a separation of up to 7 days). Overall, we conclude that QDA classifier with priors proportional to class samples in training set performed the best with an average accuracy of 83±4%.

The necessity of a narrow band spectral filter $[0.1\ 1]$ Hz suggests that anticipation related features in SCP lie in the band below 1 Hz. The high pass cut-off at 0.1 Hz effectively reduces the unrelated high amplitude ISO oscillations. Furthermore, our analysis revealed that widely used spatial filters (Laplacian filter and CAR alone) are sub-optimal for the single trial analysis of SCPs. This is likely to be due to the fact that the Laplacian filters enhances the focal activity from local sources (e.g. suitable for the mu-rhythm and low beta) and reduce broadly spread activity [9], while the SCPs are widely spatially distributed activities. To account for this nature of SCP, we proposed to use SSF that reduces high frequency spatial distribution resulting from EEG/non-EEG activity (high frequency spatial noise, artifacts). Such spatial smoothing filters are widely reported in fMRI data analysis but to the best of our knowledge never in the context of SCPs recorded using EEG [3], [10].

The results presented in the current work are very encouraging for the single trial analysis of SCP in general. However, the online real-time applicability of the methods presented here raises new challenges. Particularly, the requirement of high pass cut-off for the FIR filters for attenuating ISOs can introduce significant delays. It is worth noting that the SSF assumes symmetric distribution of SCP around a given electrode (e.g. Cz) and in reality this assumption is not fully valid (c.f. Fig. 2). To address the asymmetric nature of anticipation related SCP distribution, data driven approaches for spatial filtering similar to common spatial patterns (CSP) [12] and beamforming techniques will be investigated in future [13].

REFERENCES

[1] Niels Birbaumer, Thilo Hinterberger, Andrea Kübler, and Nicola Neumann, "The thought-translation device (TTD): Neurobehavioral mechanisms and clinical outcome.," *IEEE Trans Neural Syst Rehabil Eng*, vol. 11, pp. 120–123, 2003.

[2] Frank Schneider, Brigette Rockstroh, Hans Heimann, Werner Lutzenberger, Regina Mattes, Thomas Elbert, Niels Birbaumer, and Mathias Bartels, "Self-regulation of slow cortical potentials in psychiatric patients: Schizophrenia.," *Biofeedback Self Regul*, vol. 17, pp. 277–292, 1992.

[3] Ali Bashashati, Mehrdad Fatourechi, Rabab K Ward, and Gary E Birch, "A survey of signal processing algorithms in brain-computer interfaces based on electrical brain signals.," *J Neural Eng*, vol. 4, pp. R32–R57, 2007.

[4] Sampsa Vanhatalo, Juha Voipio, and Kai Kaila, "Full-band EEG (FbEEG): An emerging standard in electroencephalography.," *Clin Neurophysiol*, vol. 116, pp. 1–8, 2005.

[5] Garipelli Gangadhar, Ricardo Chavarriaga, and José del R Millán, "Fast recognition of anticipation-related potentials.," *IEEE Trans Biomed Eng*, vol. 56, pp. 1257–1260, 2009.

[6] Garipelli Gangadhar, Ricardo Chavarriaga, and José del R Millán, "Anticipation based brain-computer interfacing (aBCI)," in *The 4th Int IEEE EMBS Conf on Neural Eng*, 2009.

[7] Greet J. M. Van Boxtel and Koen B. E. Böcker, "Cortical measures of anticipation," *Journal of Psychophysiology*, vol. 18, pp. 61–76, 2004.

[8] Elisabeth V. C. Friedrich, Dennis J. McFarland, Christa Neuper, Theresa M. Vaughan, Peter Brunner, and Jonathan R. Wolpaw, "A scanning protocol for sensorimotor rhythm-based brain-computer interface," *Biol Psych*, vol. 80, pp. 169–175, 2009.

[9] Dennis J. McFarland, Lynn M. McCane, Stephen V. David, and Jonathan R. Wolpaw, "Spatial filter selection for EEG-based communication.," *Electroencephalogr Clin Neurophysiol*, vol. 103, pp. 386–394, 1997.

[10] Stephen C Strother, "Evaluating fMRI preprocessing pipelines," *IEEE Eng Med Biol Mag*, vol. 25, no. 2, pp. 27–41, 2006.

[11] Richard O. Duda, Peter E. Hart, and David G. Stork, *Pattern Classification*, Wiley-Interscience, 2 edition, 2000.

[12] Steven Lemm, Benjamin Blankertz, Gabriel Curio, and Klaus-Robert Müller, "Spatio-spectral filter for improved classification of single-trial EEG," *IEEE Trans Biomed Eng*, vol. 52, pp. 1541–1548, 2005.

[13] Moritz Grosse-Wentrup, Christian Liefhold, Klaus Gramann, and Martin Buss, "Beamforming in noninvasive brain-computer interfaces.," *IEEE Trans Biomed Eng*, vol. 56, pp. 1209–1219, 2009.